# Front induced transitions

**Mahmoud A. Gaafar[1,2], Toshihiko Baba[3], Manfred Eich[1,4] and Alexander Yu. Petrov[1,5]**

[1]Institute of Optical and Electronic Materials, Hamburg University of Technology, Eissendorfer Strasse 38, 21073 Hamburg, Germany
[2]Department of Physics, Faculty of Science, Menoufia University, Menoufia, Egypt
[3]Department of Electrical and Computer Engineering, Yokohama National University, 79-5 Tokiwadai, Hodogayaku, Yokohama 240-8501, Japan
[4]Institute of Materials Research, Helmholtz-Zentrum Geesthacht, Max-Planck-Strasse 1, Geesthacht, D-21502, Germany
[5]ITMO University, 49 Kronverkskii Ave., 197101, St. Petersburg, Russia

## Abstract

Moving refractive index fronts in dispersive waveguides is a special type of spatio-temporal modulation. The interaction of light with such fronts can be described in terms of an indirect transition where the frequency and wavenumber of a guided mode both are changed. In recent years front induced transitions were used in dispersion engineered waveguides for frequency conversion, optical delays, and bandwidth and pulse duration manipulation. These concepts have originated from different research areas of photonics, such as nonlinear fiber optics, slow light waveguides, plasma physics, moving media and relativistic effects. Here, we would like to review these concepts, providing a unifying theoretical description and highlight the potential of this exciting research field for light manipulation in guided optics.

## 1. Introduction

Optical waveguides are a basis for integrated and fiber optics [1-3]. The perturbation of optical parameters in space along the propagation direction leads to the changes of the wavenumber of the propagating mode [1, 4]. Such spatial perturbations can be used to engineer the accumulated phase, local group velocity and dispersion in guided systems [1, 2, 5-7]. At the same time, the temporal variation of the optical parameters lead to the change of light frequency [8-10]. Such temporal manipulations are the basis for the dynamic frequency manipulation on chip [9, 11-13]. A moving perturbation combines both spatial and temporal changes. One of the prominent moving perturbations used in photonics is a periodical one. Interacting with the guided signal it induces an indirect transition where wavenumber and the frequency of light is changed [14-16]. An example of such moving periodical perturbation is an acoustic wave which currently gains a lot of interest for realization of non-reciprocal light propagation [17, 18] and light storage [19-21]. The frequency shift in this indirect transition is limited by the modulation frequency of the perturbation. Also, due to fixed frequency and wavenumber shift, there is a strict phase matching condition that significantly limits the bandwidth of coupling [16, 17].

Here, we would like to discuss another prominent moving perturbation, namely a moving front. In recent years, several theoretical predictions and experimental demonstrations were presented where the light propagating in waveguides is manipulated by a refractive index front [22-43]. The refractive index front is produced via Kerr nonlinearity [24, 25, 35, 36] or via free carrier injection [31,

[33, 40] by a switching pulse co- or counter-propagating with respect to the signal. This refractive index perturbation is relatively weak, significantly smaller than what is observed in plasma ionization fronts for microwave and THz frequencies [44-47], where, due to large induced carrier densities, mirror like reflections are observed. Notwithstanding, the weak refractive index perturbations still induce an efficient indirect transition of the optical state similar to a periodic perturbation. Notably, the achievable frequency shift now is not limited by the temporal profile of the front but is a function of the waveguide dispersion. Also, the indirect transition induced by the front is not limited by a strict phase matching condition and, thus, can manipulate broadband signals. The dispersion engineering of the guided modes becomes a very important parameter as it defines the final state for the signal after the interaction with the front. Waveguide dispersion and front velocity can be adjusted to transmit [30, 31, 33, 42, 48-50] or reflect [24-29, 34-36, 38, 42, 43, 51] the signal or even to trap [52, 53] the signal in the front. Concepts of front induced transitions (FITs) are proposed and realized for frequency manipulation [23, 24, 35, 36, 41, 43], light stopping and optical delays [54, 55], bandwidth/time duration manipulation [30, 32, 52, 53, 56]. Reflective FITs can also represent an optical analog of an event horizon [24, 25, 35, 36, 43] and are predicted to emit an analog of Hawking radiation [24, 30, 57, 58]. Light trapping by FIT leads to a so called optical push broom effect [30, 52, 53, 59], where signal pulse can be collected inside the front.

It should be mentioned that the FITs were discussed in different areas of photonics, sometimes not directly related to each other. We unite in this review concepts that appeared in the research on slow light [13, 31, 33, 38, 39, 41, 43, 54-56], silicon photonics [9, 11, 12, 22, 35], optical analogue of event horizon [24, 25], optical solitons [42, 60-62], fiber Bragg gratings [52, 53, 59, 63], Bragg stacks [32, 64, 65], ionization fronts [44-47] and moving media [8, 48, 66]. Also different approaches were applied to explain the obtained effects, such as four wave mixing [25, 61, 62] indirect transitions in the band diagram [16, 31-33, 40, 45], geometrical optics approximation in space and time [24, 33, 38, 43], slow varying approximation leading to linear Schrödinger equation (LSE) [4, 34, 51, 67], Doppler effects [38, 64, 65].

Here, we will review the presented concepts, provide a unifying theoretical description, highlight their potential for light manipulation in guided optics, and draw an outlook for the further research in this field. The paper is organized as following: after a brief introduction to the theoretical background of FITs, we present examples of signal transmission, reflection and trapping. We will geometrically consider indirect transitions in the dispersion relation using the phase continuity relation at the front and present numerical solutions of the LSE which follows from the slowly varying envelope approximation of the wave equation. Then we discuss the concepts according to their application in frequency conversion, optical delays and bandwidth manipulation. Furthermore, we will estimate the maximal achievable effects for each of the application in different systems. We will compare the described effects with those obtained by other nonlinear phenomena, discuss advantages and disadvantages and draw the outlook.

## 2. Theory and approaches

### 2.1 The front and the dispersion

We are considering a particular moving perturbation that changes the dispersion relation of the waveguide from one before the perturbation to one after the perturbation (Fig. 1). The fronts

presented in this review were generated via either Kerr nonlinearity or free carrier generation or both. For a short pump pulse and Kerr nonlinearity, a tunnelling of the signal through the perturbation can be observed when the signal interacts with a negative front on the other side and compensates the effect [24, 29]. In order to prevent the tunnelling, a special optical pulse should be used that has a sharp leading edge [53]. On the other hand, free carrier-induced fronts have negligible negative front as free carriers typically have much longer life time than the front duration [22, 54, 68]. It should be noted that the free carriers themselves are increasing absorption losses [69]. We should also mention that the effect of the weak index perturbation can nevertheless be significant if the linear losses of the waveguide in which the index perturbation is moving is sufficiently low, allowing for long interaction distances.

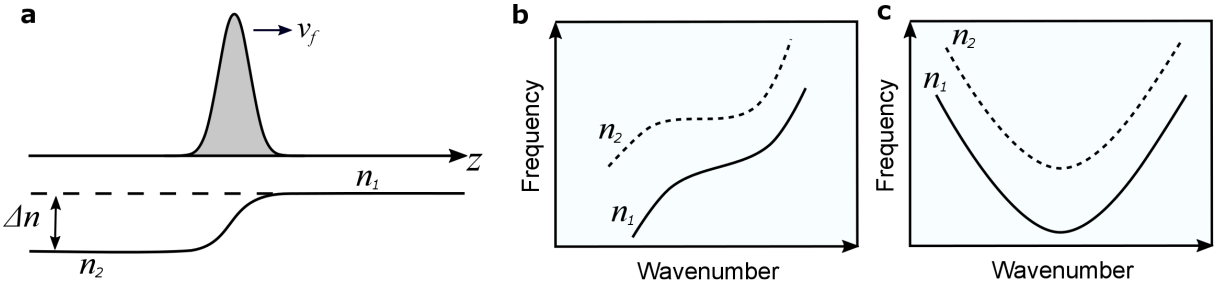


Figure 1: (a) Schematic of intense pump pulse propagation in a waveguide (up) and the corresponding induced index front (down). We consider here an example of an index front due to the effect of free carrier generation. Schematic of dispersion relations of the system before (solid curve) and after perturbation (dashed curve) as long as free carriers have not yet substantially recombined for (b) a dispersion relation close to inflection point, (c) dispersion relation close to the band edge.

A dispersion relation is a function of frequency versus wavenumber $\omega(\beta)$ or wavenumber versus frequency $\beta(\omega)$. For the discussion of front induced transitions we would prefer to use the $\omega(\beta)$ dependency as any perturbation of the dispersion relation in a static waveguide before or after the front propagation is represented by a unique frequency $\omega$ defined for any wavenumber $\beta$. Typically, the perturbation of the dispersion relation is produced by a change of dielectric constant. For a dielectric constant perturbation as a function of space $\Delta\varepsilon(\boldsymbol{r})$ for each wavenumber the frequency shift is [Ref. [70], Eq. (28)]:

$$\Delta\omega = -\frac{\omega}{2}\frac{\int \Delta\varepsilon(\boldsymbol{r})|\boldsymbol{E}(\boldsymbol{r})|^2 d\boldsymbol{r}}{\int \varepsilon(\boldsymbol{r})|\boldsymbol{E}(\boldsymbol{r})|^2 d\boldsymbol{r}}$$

Where the integration is done over the periodic unit in case of a photonic crystal waveguide or over the cross section of a continuous waveguide. If a relative perturbation $\Delta\varepsilon(\boldsymbol{r})/\varepsilon(\boldsymbol{r})$ is everywhere the same, then a vertical frequency shift of the band diagram is obtained proportional to the original frequency. In case of an inhomogeneous perturbation a geometrical distortion of the dispersion relation can be obtained (Fig. 1(b)). This distortion can be used to delay, stop or reverse light by a direct dynamic transition in a temporally varying system [9, 10, 71-74]. Such distortions are difficult to obtain as the index perturbation should vary locally. In many cases, the perturbations are close to homogeneous and just a small vertical shift of the dispersion relations is obtained (Fig. 1(c)). In this review we will limit our consideration to a vertical shift of the dispersion relation $\Delta\omega_D$ moving with constant velocity $v_f$ along the

waveguide $\Delta\omega_D(t,z) = \Delta\omega_D(z - v_f t)$. Through all examples presented in this article, we use a hyperbolic dispersion relation emulating an upper branch of a dispersion relation with a photonic band gap [52, 75] (Fig. 1(c)). We should mention that the dispersion relation near the band edge can be also approximated by a parabolic dependence. However, for the realisation of optical pushbroom effect, a hyperbolic dispersion is essential, as it converges to dispersionless behaviour away from the band edge [52, 53, 59, 63]. Furthermore, we limit our consideration to the case of weak refractive index change with smooth transition where the non-adiabatic, Fresnel-like reflection from the index front can be ignored. This is a typical situation for fronts excited by pump pulses. The band diagram shift induced by the front is described by the function $\Delta\omega_D(t) = \Delta\omega_{Dmax}/2 \cdot \left[1 + \tanh\left(1/\Delta t_f \left(t - z/v_f\right)\right)\right]$, where $\Delta t_f$ is the temporal front width and $\Delta\omega_{Dmax}$ is the maximum vertical band diagram shift in frequency. This front function is a good approximation for a front induced by a pump pulse and was used in other publications [32, 65].

**Box 1. Signal pulse interaction with a moving index front**

In case of a signal pulse propagating and interacting with the index front, its frequency and duration will change. As an example, schematic representation of signal pulse reflection at a moving front inside a periodically corrugated waveguide is shown in the figure below. The spatiotemporal change of refractive index $\Delta n$ is shown on the left, while the corrugated waveguide on the right. Here, the initial signal pulse (red colour) is counter-directed to the index front which has a finite steepness. The black arrow indicates the signal pulse trajectory. If the signal pulse cannot find states behind the front after interaction, it will reflect and therefore the new state of the signal will remain in the unchanged waveguide but with a frequency shift (blue colour).

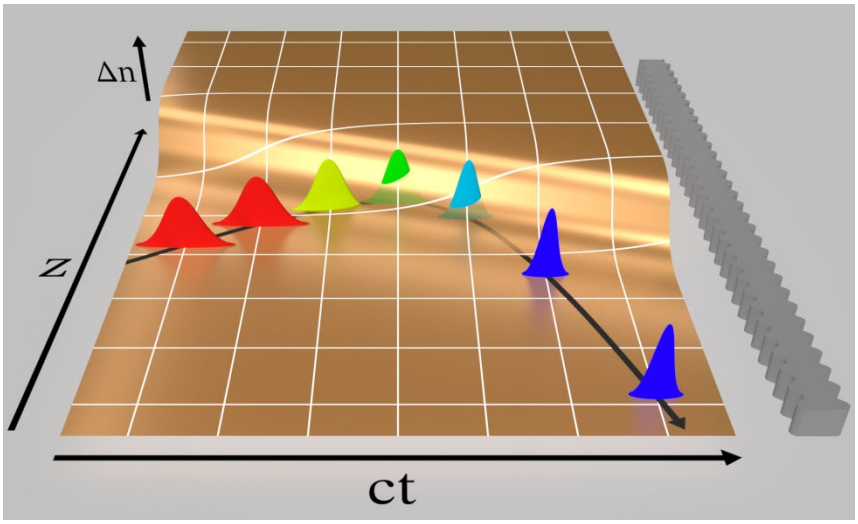

## 2.2 Indirect transitions

A schematic representation of the different FITs is illustrated in Fig. 2. Black and orange arrows represent direct and indirect transitions, respectively, while the blue arrow shows the transition due to a spatial perturbation only as is observed when a signal enters a medium and just its wavenumber changes while its frequency stays the same. Interaction with a front leads to an indirect photonic transition (orange arrow in Fig. 2(a)) with a simultaneous change of frequency and wavenumber of the optical signal [24, 31, 33]. Indirect photonic transitions between modes that belong to different photonic bands are called indirect inter-band transitions [16, 31, 33, 55], while transitions between modes that belong to the same photonic bands are called indirect intra-band transitions [38, 43]. In contrast to direct (vertical) transitions, indirect transitions create an additional method for frequency control via the choice of the transition angle, marking the straight path which connects starting and end points within the unperturbed and perturbed dispersion relations (Fig. 2).

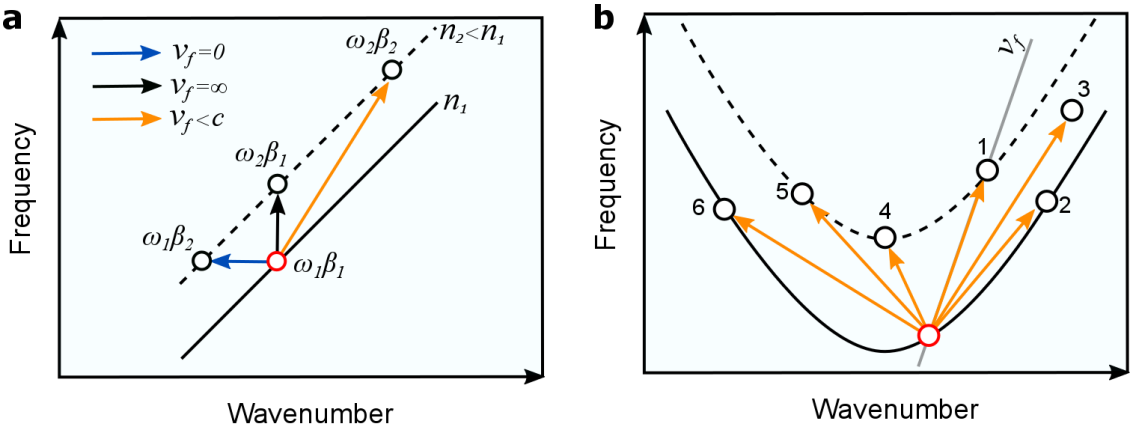


Figure 2: Schematic representation of different photonic transitions. The solid curve represents the dispersion bands of an original (unperturbed) mode, while the dashed curves indicate the switched (perturbed) state. Red and black circles indicate the initial and final state of signal wave, respectively. (a) A dispersion-free case where the unperturbed and perturbed dispersion functions are linear functions with equal slopes. Presented are: direct transition (black arrow), indirect transition (orange arrow), transition due to a spatial perturbation with no frequency shift and wavenumber shift, only (blue arrow). (b) Different indirect transitions in a highly dispersive dispersion relation by only changing the front velocity~~, only~~, which determines the direction of the transition within the dispersion diagram. 1: transmission through the front (inter-band transition), 2 and 6: reflection from a co and counter-propagating front (intra-band transitions), respectively, 3: signal trapping, 4: signal stopping, and 5 signal reversal. The initial group velocities of the front and of the signal are co-directed for transitions 1, 2 and 3, and counter directed in the transitions 4,5 and 6. The grey line represents the phase continuity line with a slope equal to the group velocity of the front (we show only one line in case 1 for clarity).

In case of a signal wave propagating and interacting with an index front, the change of its frequency and wavenumber upon interaction can be identified by assuming phase continuity at the front [31, 40, 66]. If $\omega_1, \beta_1, \omega_2, \beta_2$ denote the frequencies and wavenumbers of the signal on each side of the front, then the phase at the front is:

$$\omega_1 t - z_f \beta_1 = \omega_2 t - z_f \beta_2$$

where $z_f = v_f t$. Thus the ratio of the frequency change $\Delta\omega$ and wavenumber change $\Delta\beta$ induced by the interaction with the moving front is given by:

$$\Delta\omega/\Delta\beta = (\omega_2 - \omega_1)/(\beta_2 - \beta_1) = v_f \qquad (1)$$

This equation indicates that the ratio of the signal frequency change to the wavenumber change is identical to the velocity at which the front propagates $v_f$. Therefore, the angle of the indirect transition induced by the front is defined by the velocity of the front. We should mention that in case of a moving periodical perturbation not the ratio but the frequency and wavenumber shifts are fixed. This phase matching condition significantly limits the bandwidth of coupling in case of nonparallel dispersion bands [16, 17]. However in case of FIT, this restriction is not present and different frequency components of the input signal can accumulate different frequency shifts. FIT can project any input signal bandwidth through the phase continuity lines on the nonparallel and curved dispersion band.

Figure 2(b) shows a schematic representation of different indirect transitions in a highly dispersive system with hyperbolic dispersion as an example. The hyperbolic dispersion is a good approximation for the dispersion of a weak Bragg grating in an otherwise dispersionless waveguide [63]. Also, this kind of dispersion relation appears in periodic structures, such as photonic crystal waveguides [76], photonic crystal fibers [77], and fiber Bragg gratings [63, 75, 78]. In this schematic example, the initial group velocities of the front and of the signal are co-directed for transitions 1, 2 and 3, while are counter directed in the transitions 4, 5 and 6. The grey line represents the phase continuity line with a slope equal to the group velocity of the front/pump signal (we show only one line for clarity). The red and black circles indicate the initial and final states of the signal wave, respectively. Transitions 1 and 4 correspond to interband transitions where final states are those of the perturbed waveguide and, thus, the signal transmits through the front [31, 33]. Case 4 corresponds to a transition to a state with zero group velocity leading to the light stopping effect. Transition 2 and 6 are intraband transitions with reflection from the front in the forward [24, 25, 27, 28, 34-36, 43, 61, 62] and backward direction [27, 38], correspondingly. The transition 3 is a special case when signal does not find states in the waveguide before or after the front and thus is trapped in the front. This is the case of an optical pushbroom effect [52, 53, 59, 63]. Transition 2 and 5 are intraband and interband transitions, respectively which causes signal reversal, i.e. the time order of the incident signal is reversed. It is similar to what is obtained with direct transitions by a fast switch of the dispersion relation from positive to negative group velocity [79-83]. In transition 5, the signal spatial distribution is not reversed but signal is moving in the opposite direction after the transition leading to time reversal. In transition 2, the spatial distribution is reversed by reflection from the front, but direction of propagation stays the same, thus, again, leading to time reversal. In transition 6 there is no time reversal as spatial distribution and the direction of propagation are both reversed.

If, after the interaction with the front, the signal leaves the front region, the frequency and wavenumber changes are independent of the front profile[31, 32, 40]. In this case, a complete transition takes place, which can be completely described by projecting the initial states to final states with phase continuity line. If the length of the waveguide was insufficient for the signal to leave the front the transition is incomplete. In case of the trapping effect, independent of the waveguide length, the signal cannot leave the front and the transition is incomplete, too, and its frequency shift depends on the interaction time with the front $\Delta t$ and front slope [40, 63]:

$$\Delta\omega = \left(\frac{\partial \Delta\omega_D}{\partial t}\right)\Delta t$$

$$\Delta\beta = \Delta\omega/v_f. \quad (2)$$

2.3Slow varying envelope (SVE) approximation

Usually, the slowly varying approximation is used for the description of pulse propagation in a nonlinear medium which leads to a nonlinear Schrödinger equation [4, 34, 84, 85]. For the case of the FIT the pump effect can be described by a smooth dielectric constant $\Delta\varepsilon(r,t)$ perturbation in space and time [34, 52]. Therefore a LSE can be used. In waveguides with weak dispersion usually the spatial evolution of the pulse temporal profile is tracked [4, 34, 35, 62, 67]. In this case, the dispersion is taken into account as $\beta(\omega)$ and perturbation as $\Delta\beta(\omega)$. This is a natural choice for the comparison with experimental data as detectors are usually measuring temporal pulse profiles at certain positions in the optical signal line. However, for systems, which have non-unique dispersion relations, the $\beta(\omega)$ description and the wavenumber shift approximation become inapplicable. For example, this equation cannot be applied to the pulse propagation close to the band edge where the $\beta(\omega)$ function is not unique and the dielectric constant perturbation leads mainly to a frequency shift of the band diagram and not to a wavenumber shift. These non-unique dispersion functions appear in periodic structures [70], such as photonic crystal waveguides [76], photonic crystal fibers [77], Bragg gratings [75].

Thus, it is favorable to work with $\omega(\beta)$ representation of dispersion and with a symmetric version of a LSE where temporal evolution of the pulse spatial profile is tracked [51, 52, 59, 86]. Signal wave propagation in a dispersive waveguide with SVE function $A(t,z)$ for the carrier angular frequency $\omega_0$ and carrier wavenumber $\beta_0$ can be described by [51]:

$$\frac{\partial A(t,z')}{\partial t} = \left(v_f - v_{g0}\right)\frac{\partial A}{\partial z'} + \sum_{n=2}^{N} i^{(n+1)}\frac{\omega_n}{n!}\frac{\partial^n A}{\partial z'^n} + i\Delta\omega_D(z')A \quad (3)$$

In this equation, $\omega_n = \partial^n\omega/\partial\beta^n$ are the dispersion coefficients associated with the Taylor series expansion of the dispersion function $\omega(\beta)$ and $v_{g0}$ is the group velocity at carrier wavenumber $\beta_0$, and $z' = z - v_f t$. The front is not moving in the considered frame $(t,z')$ and thus represents a stationary perturbation where the frequency of the signal $A(t,z')$ is not changed upon interaction. Thus the interaction with the front can be well understood in this ~~corrected~~ moving frame as a signal propagating in the waveguide with a dispersion relation $\omega'(\beta) = \omega(\beta) - v_f\cdot(\beta-\beta_0)$. The temporal profile of the signal can be obtained explicitly by converting the solution back to the original frame $(t,z)$ and observing the temporal evolution at a fixed position $z$, e.g., at the waveguide output.

**Transmission through the front**

Two transmission situations are possible: either the front completely overtakes the signal, as shown in Fig. 3(a), or vice versa, the signal overtakes the front [31, 33, 48]. In both cases, the induced frequency shift of the signal is achieved upon transmission through the front, leading to an interband indirect transition either from the unshifted to the shifted band or

vice versa. Exemplary simulation results of signal pulse interaction with a co-propagating front, corresponding to the scenario in Fig. 3(a) are presented in Fig. 3(b). Under these conditions, the phase continuity line will cut through the shifted band and the signal is transmitted through the front. The dashed orange lines represent the boundaries of $\pm 2\Delta z_f$, where $\Delta z_f = v_f \Delta t_f$, while the input signal is a Gaussian pulse with duration $\tau = 4\Delta t_f$.

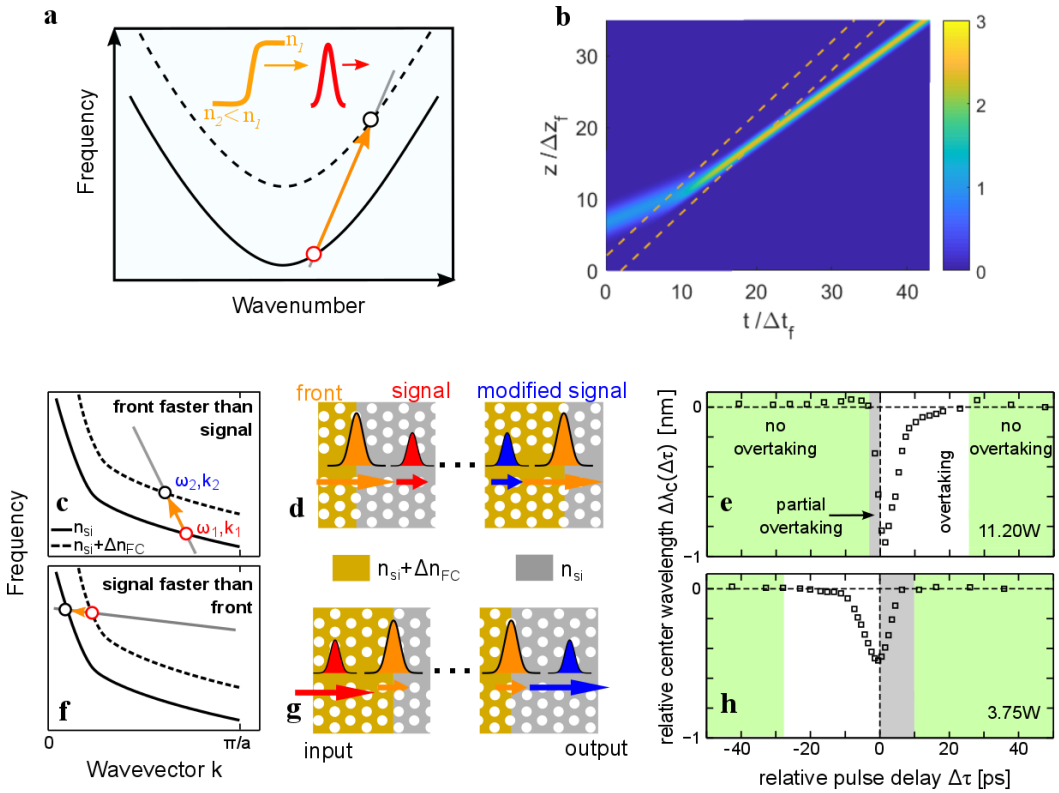


Figure 3. Signal transmission through the front: (a) Schematic representation of the transition in the band diagram. In the inset, the arrows show the initial propagation directions and group velocities of the signal (red arrow) and the front (orange arrow). The grey line represents the phase continuity line with a slope equal to the group velocity of the front $v_f = c/1.6$. (b) Temporal evolution of the signal represented in the stationary frame. The false color indicates the intensity of the electric field of the signal. (c)-(h) Experimental results of signal pulse transmission through a free carrier front in case of two different configurations:. (c); (d); (e) front faster than signal, and (f); (g); (h) signal faster than front. (a); (b) and (f); (g) schematic representation of the transitions, while (e) and (h) are the measured relative center wavelength shift as a function of delay between the signal pulse and the front for the same induced $\Delta\omega_D$. (c)-(h) Adapted from Ref. [31].

Signal pulse transmission through a moving index front has been demonstrated in silicon PhC waveguides [31, 33, 41], microwave waveguides [49, 50], and by an ionization front in a magnetized plasma [45]. Figures 3(c)-(h) presents experimental results of signal pulse transmission through a free carrier front in silicon slow light waveguide in case of two different configurations: front faster than the signal (Figs. 3(c); (d); (e)), and signal faster than the front (Figs. 3(f); (g); (h)) [31]. In case of the front completely overtaking the signal, the final state of the signal lies on the band corresponding to $n_2$ (Figs. 3(c); (d)). However, in case of the signal completely overtaking the front, the initial state of the signal lies on the switched band, while the final state lies on the original band (Figs. 3(f); (g)). The measured relative center wavelength shift as a function of delay between the signal pulse and the front for the same induced $\Delta\omega_D$ corresponding to the transitions shown in Fig.3(c), and Fig. 3(f) are shown in Fig. 3(e) and Fig. 3(h), respectively. The wavelength shift is determined by the mean spectral frequency of the shifted signal. In the

green regions of Figs. 3(e) and 3(h), the signal does not interact with the front, and therefore, no wavelength shift is observed. While in the grey regions, the front overtakes only part of the leading edge of the signal pulse in Fig. 3(e) or only the trailing edge of the signal overtakes the front in Fig. 3(h). A maximal wavelength shift is observed when signal completely transmits through the front within the slow light waveguide and thus for a slightly positive delay in case of the front taking over the signal and for a slightly negative delay when signal takes over the front. In the overtaking regime (white region) the wavelength shift decreases with larger delay as the overtaking takes place further in the waveguide, where due to linear and nonlinear losses the pump pulse already has reduced intensity. ~~A maximal wavelength shift is observed when signal transmits through the front and thus for a slightly positive delay in case of the front taking over the signal and for a slightly negative delay when signal takes over the front.~~

**Reflection at the front**

A frequency shift of the signal also can be achieved upon reflection from a co/counter propagating fronts, however only under certain conditions [24, 27, 28, 32-36, 43, 64, 65]. This can happen provided that the phase continuity line can reach the final state on the same band without cutting into the shifted band, as shown in Fig. 4(a). The phase continuity line #1 is shown for a co-propagating front and #2 for a counter-propagating front. This intraband transition manifests itself as a forward/backward reflection from the co-propagating [24, 25, 28, 32, 34-36, 43, 50, 62, 67] and counter-propagating [27, 32, 38, 51, 64, 65] fronts, respectively. The reflection was demonstrated experimentally by employing either the Kerr effect [24, 25, 35] or two photon absorption-induced free carriers [43].

Figure 4(b) presents the simulation result of a signal pulse interaction with a co-propagating front, corresponding to the scenario #1 in Fig. 4(a). As we can see in Fig. 4(b), the signal pulse penetrates the front up to a position where its group velocity has gradually increased until matching that of the front. After that, the signal pulse starts to recede from the front, in the forward direction, as its group velocity increases and it finally escapes (forward reflection). In this case also time reversal of the signal is obtained.

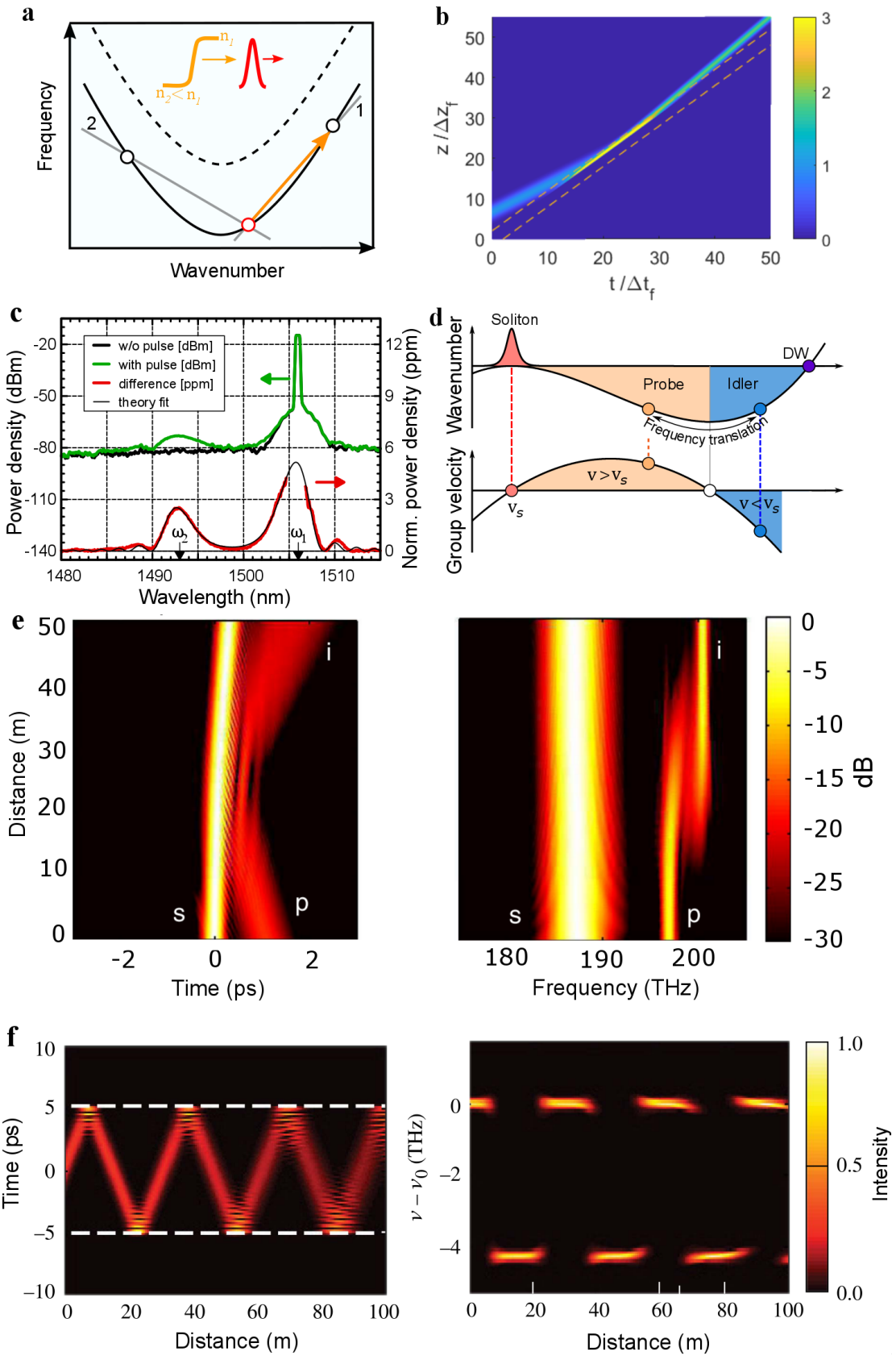


Figure 4. Signal reflection from the front: (a) Schematic representation of the transition in the band diagram. Here, the signal and the front counter-propagating as shown in the inset. The group velocity of the front is $c/3.6$. (b) Temporal evolution of the same signal represented in the stationary frame. The false color indicates the intensity of the electric field of the signal. (c) Experimental results of signal light reflection and blue-shifting at a co-propagating Kerr induced index front in a fiber. The black curve shows the power spectrum of signal light that has not interacted with the front, whereas the green curve displays the result of the

interaction. The difference between the spectra on a linear scale, shown in red color, exhibits a peak around the blue-shifted wavelength $\omega_2$ and another peak around the spectral line of the signal light $\omega_1$. Adapted from Ref. [24]. (d) Wavenumber and corresponding laboratory-frame group velocity plotted as a function of frequency. Phase-matched signal (probe)-idler pairs experience group velocities with opposite signs relative to the pump pulse (soliton). Waves whose frequencies lie in the orange (blue)-shaded area propagate faster (slower) than the soliton. (e) The temporal and corresponding spectral evolution of a soliton pump and probe pulse in an optical fiber (p = probe , s = soliton , i = idler). In the time domain, the probe appears to reflect off the soliton, owing to the generation of an idler. (d) and (e) adapted from Ref. [25]. (f) Temporal (left) and spectral (right) evolution of signal pulse reflected from a pair of fronts with positive and negative slopes acting as a temporal analog of planar dielectric waveguide. Adapted from Ref. [67].

Figure 4(c) presents the experimental results of signal wave reflection at a Kerr-induced co-propagating front in a silica fiber [24]. The black curve shows the power spectrum of a CW signal light that has not interacted with the front, whereas the green curve displays the result of the interaction. The difference between the spectra on a linear scale, shown in red color, exhibits a peak around the blue-shifted wavelength $\omega_2$ and another peak around the spectral line of the signal light $\omega_1$. The blue shifted peak is a portion of the CW signal that was reflected by the front and the peak at the initial frequency corresponds to frequency components of a temporal 'shadow' left inside the CW signal after the cut-out of the wavepackets interacting with the front. The side lobes are a diffraction effect due to rectangular shape of the converted signal and the 'shadow'. Though the refractive index change in the glass fiber was in the order of $10^{-6}$, only, a large wavelength shift of 13 nm (in the order of 1 %) is obtained due to the indirect intraband transition. This effect, as we mentioned before, is also considered as an optical analogue of an event horizon where light cannot leave the space on one side of the front [24, 87]. In fibers usually a $\beta(\omega)$ dispersion representation is used and a corrected time frame $t' = t - z/v_f$. In this ~~corrected~~ moving frame a band diagram is $\beta'(\omega) = \beta(\omega) - 1/v_f(\omega - \omega_0)$ and the front is everywhere the same, representing a time perturbation only [34]. Fig. 4(d) shows the dispersion relation of the fiber, as well as the corresponding laboratory-frame group velocity [25]. While Fig. 4(e) presents the temporal and corresponding spectral evolution of a pump (soliton) and a weak signal (probe) pulse propagating in the fiber [25]. We can see from Fig. 4(d) that a signal-idler pair will experience group velocities of opposite sign relative to the pump. This means that, when interacting with the pump, a signal travelling faster than the pump will be converted into an idler travelling slower than the pump, and vice versa. In the reference frame of the pump, the frequency conversion therefore gives rise to a reflection of the signal off the pump, as shown in Fig. 4(e). Fronts were also predicted to emit an analog of Hawking radiation in optical fiber waveguides [24, 57, 58], cavities [30], or ultrashort laser pulse filaments [88].

A pair of fronts with opposite sign of the slope separated in time can be also used to confine light [67, 89]. In this case such boundaries act as a temporal analog of planar dielectric waveguides. Figure 4(f) present the temporal (left) and spectral (right) evolution of pulse reflection from such boundaries. Discrete modes of such temporal waveguides can be defined and excited [67, 89].

The dispersive wave launching used for supercontinuum generation [90] also bears similarity to the reflection from a refractive index front. In this case part of the soliton energy is accelerated or decelerated by the own refractive index modulation. An ionization front was used, for example, to extend the supercontinuum generation in gas-filled photonic crystal fiber to mid-infrared range [91].

A special type of the reflecting front is a front of a photonic band gap. In this case the band diagram is not just shifted, but degeneracy between forward and backward propagating waves is lifted and a band gap is opened. The FITs at such front were predicted theoretically and demonstrated by simulation in Ref. [32, 64, 65]. It has been shown, that when the center frequency of an incident signal pulse lies at the center of the photonic band gap, pulse compression/broadening are observed when it counter/co-propagates with the moving front, respectively without change of the center frequency [32]. Very strong shock fronts that significantly perturb the dispersion relation can even trap signals in the front [64] or provide inverse Doppler shifts [65].

**Trapping inside the front**

The signal can also undergo neither inter nor intra-band transitions and be trapped inside the front, as shown schematically in Fig. 5(a). This happens when the phase continuity line does not cut the unperturbed (solid black) and the completely perturbed (dashed black) dispersion curve. Before the approaching index front encounters the signal pulse, the signal moves along a straight line with constant group velocity $v_{g1}$. Upon contact with the front, the signal will be gradually frequency shifted along the phase continuity line, and correspondingly gradually accelerated, by the front until its velocity reaches the velocity of the front $v_{g2} = v_f$ and stays trapped inside it.

Simulation results of this phenomenon are presented in Fig. 5(b). The signal pulse will be compressed in time and space inside the front (see Fig. 5(b)) which is also accompanied by strong frequency broadening. Interesting is that the corrected dispersion relation $\omega'(\beta) = \omega(\beta) - v_f \cdot (\beta - \beta_0)$ in case of trapping represents a saturating function with zero group velocity at infinite wavenumber $\beta$. It reminds the dispersion relation of a surface plasmon polariton [92]. When a surface plasmon polariton encounters a tapered perturbation that does not allow further propagation then it is not reflected but is trapped at the transition leading to nanofocusing effects [93, 94]. The same is obtained now in a moving front in a medium with hyperbolic dispersion curve $\omega(\beta)$.

Such signal pulse trapping in the front has been theoretically proposed [52, 59, 63] and experimentally realized in a fiber Bragg grating [53], named as optical pushbroom effect. In the experiment with fiber Bragg gratings a special optical pulse was used to generate a sharp front via Kerr nonlinearity [53]. Due to a small shift of the dispersion relation in the fiber as well as due to the small velocity mismatch between front and signal pulse, only a small compression factor of 5 has been demonstrated (Figs. 5(c),(d)), Namely, the front has compressed an approximately 500 ps portion of a CW signal into a 70 ps pulse. Using the same effect Eilenberger *et. al.* showed that light trapped in an optical cavity of a fiber Bragg grating can be extracted from that cavity in an ultrashort burst by means of an ultrafast intense pump pulse acting like a shock-front propagating through the cavity [30] (see Fig. 5(e),(f)). The energy in the cavity has different wavevectors and is projected by phase continuity line on the photonic bands above and below bandgap. The new excited frequencies co-propagate with the pump pulse. They have frequencies above or below the band gap and thus are released from the cavity.

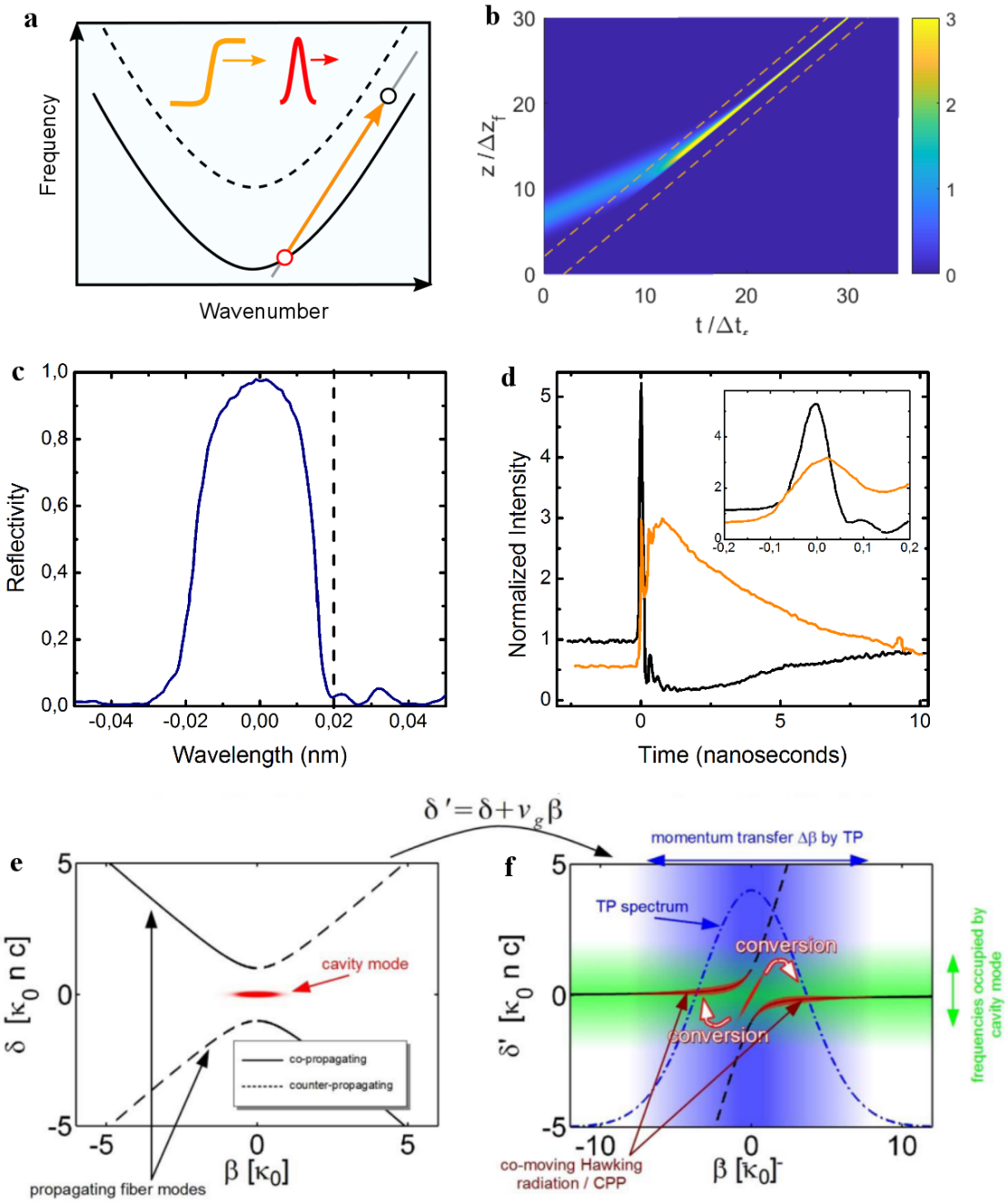


Figure 5. Signal trapping inside the front: (a) Schematic representation of the transition in the band diagram. In the inset, the arrows show the initial propagation directions and group velocities of the signal (red arrow) and the front (orange arrow). The group velocity of the front is $c/2$. (b) Temporal evolution of the same signal represented in the stationary frame. The false color indicates the intensity of the electric field of the signal. (c) and (d) Experimental results of optical pushbroom in a fiber Bragg grating waveguide. (c) The measured reflection spectrum of the fiber Bragg grating used in the experiment. The dashed vertical line indicates the initial frequency of the signal. (d) The solid line shows the intensity of the signal light as a function of delay between the signal and front. The intensity of the signal light is normalized so that the transmitted power in the absence of the grating would be unity. The dashed line represents the transmitted pump pulse power that constitutes the front. The inset shows a zoomed in view of the front peak. 5 times intensity enhancement corresponds to approximately 5 times pulse compression. Adapted from Ref. [53].(e) and (f) light trapped in an optical cavity can be extracted from that cavity in an ultrashort burst by means of an ultrafast intense pump pulse acting like a shock-front propagating through the cavity. (e) and (f) are adapted from [30].

## 3. Applications

3.1 Frequency conversion

As we discussed above, several contributions have experimentally demonstrated signal frequency conversion with FITs [24, 25, 31, 33, 35, 41]. The coherent frequency manipulation of optical signals might play an important role in different areas, such as wavelength-division multiplexing (WDM) based optical communication [95] and quantum communication [96]. According to Eq. (2) FIT of a signal at 200 THz (1550 nm) with dispersion shift of $\omega_D = 100$ Hz (0.75 nm), front duration of $\Delta t_f = 1$ ps and interaction time of $\Delta t = 100$ ps in an integrated waveguide can induce a frequency shift of 10 THz (75 nm). Currently, the maximal wavelength shift of 84 nm was achieved in 22 mm silicon strip waveguides [35]. A blue shift of a few nanometers is also obtained in PhC waveguides [31, 33], while a sub-nm red shift is demonstrated by dynamic carrier depletion using p-i-n diode [41]. The fibres can provide much longer interaction time but usually have smaller nonlinearity. A wavelength shift of 13 nm was realised in a 1.5 m photonic crystal fibre [24]. The quantum conversion efficiency of FIT can approach 100% if the front does not introduce additional absorption. In fibres a conversion efficiency of 10% was demonstrated, limited by the transmission through the Kerr induced perturbation [24]. The free carrier induced front showed up to 30% efficiency, limited by free carrier absorption [43].

The frequency shift induced by FIT has advantages in comparison to that induced by copropagating cross phase modulation (XPM) and compared to idler generation in four wave mixing (FWM) configurations. In contrast to XPM and FWM [97-99] the FITs function with large group velocity mismatch between signal and pump. Further, in FWM, the pump frequency always has to lie between signal frequency and idler frequency thus, if positioned in relatively narrow frequency band, causing a cross-talk, which is especially a problem for WDM systems. In case of FIT and XPM the front/pump can be positioned outside of the signal frequency window.

Furthermore, in contrast to FWM and XPM, the signal shifted by FIT does not need to have the pulsed nature of the pump pulse, as front can convert a long portion of information. The shifted signal duration depends on both the group velocity differences between the pump and the signal and on the interaction length $L$ which is limited by the device length:

$$\tau_{shifted} = L\left(\frac{\left|n_g^s - n_g^f\right|}{c}\right)$$

Thus, with a front large portions of signal can be shifted in one step, for example a whole packet of binary optical signal information using a short pump pulse. As an example, if we assume a 1mm long slow light waveguide and a group index difference between the pump and the signal of 30, then the time span of the converted signal by the front will be 100 ps. Thus FIT can profit from large index change of short pulses but is not limited by the time duration of these pulses. The complete FITs are not dependent on the slope of the front rising edge but depend only on the initial and final states. Thus, the exact shape of the pump pulse generating the front is not important. Additionally, the complete indirect intra-band transitions are defined by the

unperturbed band and group velocity of the front only. Thus, the perturbed band does not influence the transition anymore and the frequency shift becomes also independent of the pump power.

Here, we have considered smooth fronts and applied slowly varying approximation to describe interactions. Adiabatic frequency conversion in a dynamical system occur when an external perturbation of the system varies slowly in space and time compared to its frequency and wavelength, allowing the system to adapt to the external changes [8, 100]. In FITs the adiabatic process occurs when the length over which the front rises is much larger than the wavelength and its duration is much longer than the optical oscillation. On the other hand, when the external perturbation of the system varies very fast, this constitutes an abrupt, highly non-adiabatic change in system parameters. Consequently, the system does not remain at one of its eigenmodes, rather, multiple eigenmodes are excited and superpose. Non-adiabatic frequency conversion using sharp fronts have been discussed [32, 38, 45, 65]. The phase continuity line still applies, but now, also states on multiple dispersion curves, corresponding to higher order or lower order modes, can be excited. The transition efficiency from the initial state to individual modes depends on the mode overlap between initial and final states weighted by the perturbation function. This way much larger frequency shifts can be obtained but at a cost of lower efficiency.

### 3.2 Bandwidth/time duration manipulation

Compression or stretching of transform limited pulses involves frequency manipulation. Optical pulse temporal compression has been theoretically discussed and experimentally demonstrated using different approaches in the last years [101]. A FWM [102], XPM [37] or electrooptic modulation [103] induced time lenses were used to build a temporal telescope with compression factors up to 27 [102]. Such time lenses require specially prepared pump pulses or fast electrooptic modulation and adjusted dispersion compensation elements. Spectral bandwidth compression has been also envisaged by direct transitions with fast tilting of the dispersion relation of the waveguide where signal pulse is propagating [13, 56, 71, 73]. At the same time significant tilting of the dispersion relation requires strong and spatially varying changes of the refractive index.

The pulse compression with FITs can be split into two categories: via complete (transmission or reflection) and incomplete transitions (trapping). The complete indirect transitions allow the projection to the part of the dispersion relation with a different slope without requirement for strong change in the shape of the dispersion relation [32]. From this geometrical consideration the temporal compression factor can be derived as $\left[(v_f/v_{g2} - 1)/(1 - v_f/v_{g1})\right]$, where $v_{g1}$ and $v_{g2}$ are the group velocities of the signal before and after the interaction with the front [51, 66]. The compression factor will increase when the front velocity $v_f$ will approach the group velocity of the final state $v_{g2}$. Significant pulse compression was not realized so far with FITs involving reflection or transmission. In case of trapping the accumulated frequency shift is proportional to the time spend inside the front (see Eq. (2)), different parts of the signal automatically accumulate a linear chirp in frequency according to the time when they enter the

front. This way, the signal time function is directly converted to frequency function, where the frequency distribution has a width equal to $(\Delta\omega_D/\Delta t_f)\tau$, where $\tau$ is the pulse duration. For the band diagram shift $\Delta\omega_D$ corresponding to 1 nm wavelength shift, front duration of $\Delta t_f = 1$ ps and signal of 100 ps the bandwidth can approach 100 nm. If the dispersion is compensated and a transform limited pulse is obtained then the compression factor of 3000 can be expected. Up to now only 5 times pulse compression was demonstrated using fibre Bragg gratings as dispersive waveguides [53]. The compression was limited by a weak nonlinearity of the silica fibre and long front duration of 30 ps.

A special situation is created by the frequency shift with a decaying front [39]. In this case, the front induces a complete transition with a decaying frequency shift along the waveguide. Thus, the signal pulse accumulates a frequency chirp. The signal can be simultaneously compressed by introducing an additional linear chirp in the waveguide. A compression factor of approximately 10 times was realized [39].

### 3.3 Light storage and optical delays

Dynamic storing and delaying optical signals offer new possibilities in all-optical processing and enhanced light-matter interactions. Therefore, this field has been driven by a variety of research efforts in past years [19, 54, 104-106]. Light storage and release by direct transition in photonic waveguides has been theoretically proposed by Yanik *et. al.* [10, 71]. In this case, the dispersion relation is modified to have zero slope in a switched state and the signal bandwidth ideally collapses to a single frequency. To release the signal the system should be switched back to the original dispersion relation. Such strong modification of the dispersion relation requires fast and strong local refractive index changes [71, 74] which are difficult to achieve [56]. Thus, several studies experimentally demonstrated similar operation by controlling the Q factor in a single cavity or coupled cavities [104, 107-110]. First demonstration of storing light on-chip was obtained in two ring resonators with a storage time of approximately 200 ps [104]. Upham *et al.* demonstrated a dynamic capture of 4 ps optical pulse inside a gallium arsenide photonic crystal nanocavity with negligible absorption losses, due to the short carrier lifetime of ~ 7 ps [110]. The limitation of the dynamic storage in the cavity is the amount of stored information. Namely, only a single pulse can be stored but not a sequence of pulses.

On the other hand, light stopping can be realized in waveguides by inducing indirect photonic transitions to point of zero group velocity (Fig. 2(b), transition 4), which was not discussed so far. The storage time will be limited by the residual dispersion at zero group velocity point. This approach is probably more feasible than the band tilting in a direct transition and would allow storing a sequence of pulses in the waveguide [10]. The signal can be later released by a front with an opposite slope. In PhC waveguides a storage of ≈ 20 ps was realized in a two step transition [55]. Alternatively a special chirped PhC waveguide with ≈ 10 ps dynamic delay was realized (Fig. 6) [54]. In the chirped structure the dispersion relation has a flat band dispersion relation (see Fig. 6(c)). The signal pulse transmits through the structure, gradually changing its wavenumber from the point before the flat band to the point behind the flat band. In the middle of the structure the signal is strongly slowed down and thus accumulates large optical delay. A control pulse generating the front runs over the signal. Due to the nature of the indirect transition it shifts the

signal to smaller wavenumbers in the band diagram Fig. 6(c) and allows for the signal to be faster released from the flat band region. Depending on the delay between the signal and control pulse the release time can be controlled and thus the accumulated delay.

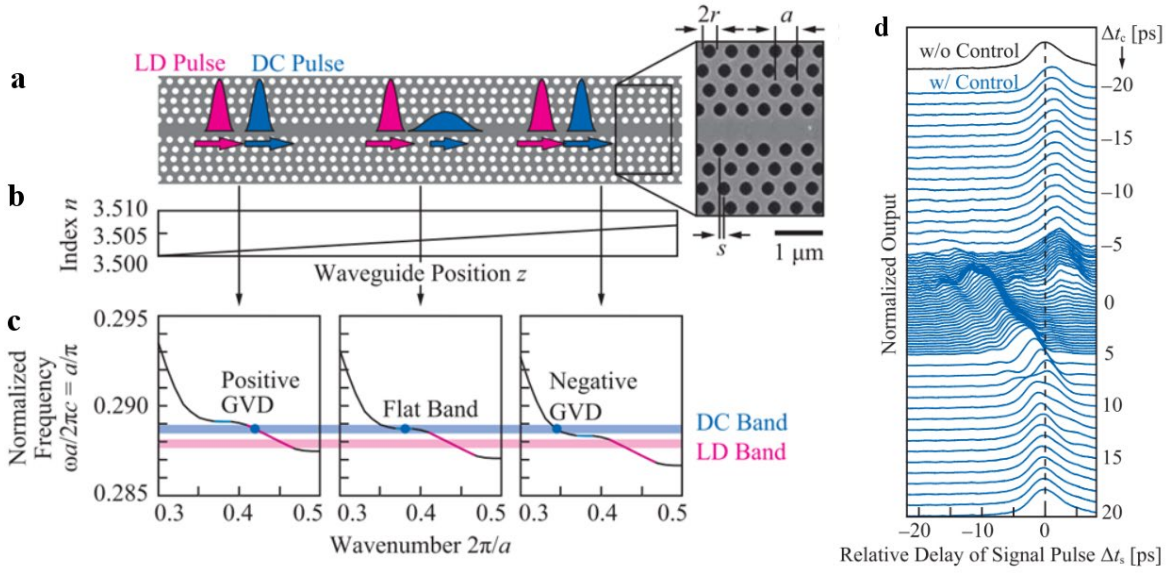


Figure 6: Dynamic pulse delay in a PhC waveguide. (a) Schematic of the structure (left) and scanning electron micrograph of fabricated device (right). Pink color indicates the pump pulse, while blue color indicates the signal pulse. LD means low-dispersion, while DC means dispersion-compensated. The arrows indicate the group velocities. (b) Schematic of the index chirp. (c) An example of calculated photonic bands assuming the index chirp in (b). (d) The relative delay of output signal pulse $\Delta t_s$ at different incident timings of the front $\Delta t_c$. Here, $\Delta t_c = 0$ corresponds to the pump (front) and signal pulses being incident simultaneously, and $\Delta t_c > 0$ is when the pump pulse is incident later. Adapted from Ref. [54].

## 4. Conclusion and outlook

A moving front in an optical waveguide usually induces only a small perturbation of the dispersion relation. But even this small perturbation combined with the dispersion of the waveguide and adjusted front velocity can be utilized to demonstrate a palette of optical interactions. Due to the fact that front induces an indirect transition that changes both frequency and wavenumber of a signal, even weak fronts can reflect or trap light.

The application of FIT has two fundamental advantages in comparison to other established nonlinear interactions in guided media. First, the FIT is not directly related to the frequency and phase of the switching pulse as the refractive index modulation is a function of intensity, only. Thus, the switching pulse center frequency can be chosen far away from the signal window which strongly reduces crosstalk from the switching to the signal channel. Second, due to the indirect nature of FIT transitions large frequency shifts can be achieved even with small refractive index changes and transitions to states with very different group velocities or even a transition to zero or negative group velocity is possible. With an indirect transition the FIT provides the full freedom of frequency and wavenumber manipulation for signal processing. FITs show also the potential for realizing frequency conversion of quantum light, such as single photons [37].

The FIT has strong potential for light manipulation in guided optics and many new concepts can be developed and existing concepts experimentally realized. Non-adiabatic transitions and fronts moving with varying velocity can be a further extension of the topic. We hope this review will allow for better understanding of FIT phenomena and pave the way for new FIT applications on chip. The review stayed in realm of classical electrodynamics. Better understanding of classical phenomena can also lead to the developments of front induced quantum effects, like the optical analog of Hawking radiation [24, 30, 58, 88, 111].

**Acknowledgements**

We would like to acknowledge the support of the German Research Foundation (DFG) under Grant No. 392102174. We further acknowledge the discussion with Hagen Renner.

**Author Contributions**

M.G. performed the LSE simulations and wrote the first draft of the manuscript with A.Y.P. All authors discussed and edited the content in the manuscript.

**Competing Interests**

The authors declare no competing interests.

## References

1. Snyder AW, Love J. *Optical Waveguide Theory*. Springer, Boston, MA, 1983.

2. Laurent Vivien LP. *Handbook of Silicon Photonics* 1st edn. CRC Press, 2013.

3. Cheben P, Halir R, Schmid JH, Atwater HA, Smith DR. Subwavelength integrated photonics. *Nature* 2018, **560**(7720)**:** 565-572.

4. Agrawal GP. *Nonlinear fiber optics*, 5 edn. Academic, Boston, 2013.

5. Baba T. Slow light in photonic crystals. *Nat. Photon.* 2008, **2**(8)**:** 465-473.

6. Krauss TF. Why do we need slow light? *Nat. Photon.* 2008, **2:** 448.

7. Priolo F, Gregorkiewicz T, Galli M, Krauss TF. Silicon nanostructures for photonics and photovoltaics. *Nat. Nanotechnol.* 2014, **9:** 19.

8. Stepanov NS. Adiabatic transformation of a wave spectrum in a nonstationary medium with dispersion. *Radiophys. Quantum Electron.* 1969, **12**(2)**:** 227-234.

9. Geltner I, Avitzour Y, Suckewer S. Picosecond pulse frequency upshifting by rapid free-carrier creation in ZnSe. *Appl.Phys. Lett.* 2002, **81**(2)**:** 226-228.

10. Yanik MF, Fan S. Stopping Light All Optically. *Phys. Rev. Lett.* 2004, **92**(8)**:** 083901.

11. Notomi M, Mitsugi S. Wavelength conversion via dynamic refractive index tuning of a cavity. *Phy.Rev. A* 2006, **73**(5)**:** 051803.

12. Upham J, Tanaka Y, Asano T, Noda S. On-the-Fly Wavelength Conversion of Photons by Dynamic Control of Photonic Waveguides. *Appl.Phys. Exp.* 2010, **3**(6)**:** 062001.

13. Castellanos Muñoz M, Petrov AY, Eich M. All-optical on-chip dynamic frequency conversion. *Appl.Phys. Lett.* 2012, **101**(14)**:** 141119.

14. Kim BY, Blake JN, Engan HE, Shaw HJ. All-fiber acousto-optic frequency shifter. *Opt. Lett.* 1986, **11**(6)**:** 389-391.

15. Stolte R, Ulrich R. Integrated-optical gigahertz frequency shifter for 1.5 µm signals. *Electron. Lett.* 1997, **33**(14)**:** 1217-1219.

16. Yu Z, Fan S. Complete optical isolation created by indirect interband photonic transitions. *Nat. Photon.* 2009, **3**(2)**:** 91-94.

17. Kittlaus EA, Otterstrom NT, Kharel P, Gertler S, Rakich PT. Non-reciprocal interband Brillouin modulation. *Nat. Photon.* 2018, **12**(10)**:** 613-619.

18. Sounas DL, Alù A. Non-reciprocal photonics based on time modulation. *Nat. Photon.* 2017, **11**(12)**:** 774-783.

19. Zhu Z, Gauthier DJ, Boyd RW. Stored Light in an Optical Fiber via Stimulated Brillouin Scattering. *Science* 2007, **318**(5857)**:** 1748-1750.

20. Merklein M, Stiller B, Vu K, Madden SJ, Eggleton BJ. A chip-integrated coherent photonic-phononic memory. *Nat. Commun.* 2017, **8**(1)**:** 574.

21. Merklein M, Stiller B, Eggleton BJ. Brillouin-based light storage and delay techniques. *J. Opt.* 2018, **20**(8)**:** 083003.

22. Dekker R, Driessen A, Wahlbrink T, Moormann C, Niehusmann J, Först M. Ultrafast Kerr-induced all-optical wavelength conversion in silicon waveguides using 1.55 µm femtosecond pulses. *Opt. Exp.* 2006, **14**(18)**:** 8336-8346.

23. Hsieh IW, Chen X, Dadap JI, Panoiu NC, Osgood RM, McNab SJ*, et al.* Cross-phase modulation-induced spectral and temporal effects on co- propagating femtosecond pulses in silicon photonic wires. *Opt. Exp.* 2007, **15**(3)**:** 1135-1146.

24. Philbin TG, Kuklewicz C, Robertson S, Hill S, König F, Leonhardt U. Fiber-Optical Analog of the Event Horizon. *Science* 2008, **319**(5868)**:** 1367.

25. Webb KE, Erkintalo M, Xu Y, Broderick NGR, Dudley JM, Genty G*, et al.* Nonlinear optics of fibre event horizons. *Nat. Commun.* 2014, **5:** 4969.

26. Lobanov VE, Sukhorukov AP. Total reflection, frequency, and velocity tuning in optical pulse collision in nonlinear dispersive media. *Phy.Rev. A* 2010, **82**(3)**:** 033809.

27. Rosanov NN, Vysotina NV, Shatsev AN. Forward light reflection from a moving inhomogeneity. *JETP Lett.* 2011, **93**(6)**:** 308-312.

28. Sukhorukov AP, Voitova TA, Lobanov VE, Bugai AN, Sazonov SV. Nonlinear effects upon collisions of optical pulses: Tunneling, blocking, and trapping. *Bull. Russ. Acad. Sci.: Physics* 2012, **76**(3)**:** 305-308.

29. Choudhary A, König F. Efficient frequency shifting of dispersive waves at solitons. *Opt. Exp.* 2012, **20**(5)**:** 5538-5546.

30. Eilenberger F, Kabakova IV, de Sterke CM, Eggleton BJ, Pertsch T. Cavity Optical Pulse Extraction: ultra-short pulse generation as seeded Hawking radiation. *Sci.Rep.* 2013, **3:** 2607.

31. Castellanos Muñoz M, Petrov AY, O'Faolain L, Li J, Krauss TF, Eich M. Optically Induced Indirect Photonic Transitions in a Slow Light Photonic Crystal Waveguide. *Phys. Rev. Lett.* 2014, **112**(5)**:** 053904.

32. Ulchenko EA, Jalas D, Petrov AY, Muñoz MC, Lang S, Eich M. Pulse compression and broadening by reflection from a moving front of a photonic crystal. *Opt. Exp.* 2014, **22**(11)**:** 13280-13287.

33. Kondo K, Baba T. Dynamic Wavelength Conversion in Copropagating Slow-Light Pulses. *Phys. Rev. Lett.* 2014, **112**(22)**:** 223904.

34. Plansinis BW, Donaldson WR, Agrawal GP. What is the Temporal Analog of Reflection and Refraction of Optical Beams? *Phys. Rev. Lett.* 2015, **115**(18)**:** 183901.

35. Ciret C, Leo F, Kuyken B, Roelkens G, Gorza S-P. Observation of an optical event horizon in a silicon-on-insulator photonic wire waveguide. *Opt. Exp.* 2016, **24**(1)**:** 114-124.

36. Kanakis P, Kamalakis T. Enabling transistor-like action in photonic crystal waveguides using optical event horizons. *Opt. Lett.* 2016, **41**(7)**:** 1372-1375.

37. Matsuda N. Deterministic reshaping of single-photon spectra using cross-phase modulation. *Sci. Adv.* 2016, **2**(3).

38. Kondo K, Baba T. Slow-light-induced Doppler shift in photonic-crystal waveguides. *Phy.Rev. A* 2016, **93**(1)**:** 011802.

39. Kondo K, Ishikura N, Tamura T, Baba T. Temporal pulse compression by dynamic slow-light tuning in photonic-crystal waveguides. *Phy.Rev. A* 2015, **91**(2)**:** 023831.

40. Gaafar MA, Petrov AY, Eich M. Free Carrier Front Induced Indirect Photonic Transitions: A New Paradigm for Frequency Manipulation on Chip. *ACS Photonics* 2017, **4**(11)**:** 2751-2758.

41. Kondo K, Baba T. Adiabatic wavelength redshift by dynamic carrier depletion using p-i-n-diode-loaded photonic crystal waveguides. *Phy.Rev. A* 2018, **97**(3)**:** 033818.

42. Marest T, Mas Arabí C, Conforti M, Mussot A, Milián C, Skryabin DV*, et al.* Collision between a dark soliton and a linear wave in an optical fiber. *Opt. Exp.* 2018, **26**(18)**:** 23480-23491.

43. Gaafar MA, Jalas D, O'Faolain L, Li J, Krauss TF, Petrov AY*, et al.* Reflection from a free carrier front via an intraband indirect photonic transition. *Nat. Commun.* 2018, **9**(1)**:** 1447.

44. Semenova VI. Reflection of electromagnetic waves from an ionization front. *Radiophys. Quantum Electron.* 1967, **10**(8)**:** 599-604.

45. Lai CH, Katsouleas TC, Mori WB, Whittum D. Frequency upshifting by an ionization front in a magnetized plasma. *IEEE T. Plasma Sci.* 1993, **21**(1)**:** 45-52.

46. Lampe M, Ott E, Walker JH. Interaction of electromagnetic waves with a moving ionization front. *Phys. Fluids* 1978, **21**(1)**:** 42-54.

47. Meng F, Thomson MD, Roskos HG. Relativistic Doppler frequency upconversion of terahertz pulses reflecting from a photoinduced plasma front in silicon. *Phy.Rev. B* 2014, **90**(15)**:** 155207.

48. Biancalana F, Amann A, Uskov AV, O'Reilly EP. Dynamics of light propagation in spatiotemporal dielectric structures. *Phy.Rev. E* 2007, **75**(4)**:** 046607.

49. Savage RL, Joshi C, Mori WB. Frequency upconversion of electromagnetic radiation upon transmission into an ionization front. *Phys. Rev. Lett.* 1992, **68**(7)**:** 946-949.

50. Savage RL, Brogle RP, Mori WB, Joshi C. Frequency upshifting and pulse compression via underdense relativistic ionization fronts. *IEEE T. Plasma Sci.* 1993, **21**(1)**:** 5-19.

51. Mahmoud A. Gaafar HR, Alexander Yu. petrov, and Manfred Eich. Linear Schrödinger equation with temporal evolution for front induced transitions *arXiv:190102191* 2019.

52. de Sterke CM. Optical push broom. *Opt. Lett.* 1992, **17**(13)**:** 914-916.

53. Broderick NGR, Taverner D, Richardson DJ, Ibsen M, Laming RI. Optical Pulse Compression in Fiber Bragg Gratings. *Phys. Rev. Lett.* 1997, **79**(23)**:** 4566-4569.

54. Kondo K, Shinkawa M, Hamachi Y, Saito Y, Arita Y, Baba T. Ultrafast Slow-Light Tuning Beyond the Carrier Lifetime Using Photonic Crystal Waveguides. *Phys. Rev. Lett.* 2013, **110**(5)**:** 053902.

55. Beggs DM, Rey IH, Kampfrath T, Rotenberg N, Kuipers L, Krauss TF. Ultrafast Tunable Optical Delay Line Based on Indirect Photonic Transitions. *Phys. Rev. Lett.* 2012, **108**(21)**:** 213901.

56. Beggs DM, Krauss TF, Kuipers L, Kampfrath T. Ultrafast Tilting of the Dispersion of a Photonic Crystal and Adiabatic Spectral Compression of Light Pulses. *Phys. Rev. Lett.* 2012, **108**(3)**:** 033902.

57. Jacquet M, König F. Quantum vacuum emission from a refractive-index front. *Phy.Rev. A* 2015, **92**(2)**:** 023851.

58. Bermudez D, Leonhardt U. Hawking spectrum for a fiber-optical analog of the event horizon. *Phy.Rev. A* 2016, **93**(5)**:** 053820.

59. Steel MJ, Jackson DGA, Martijn de Sterke C. Approximate model for optical pulse compression by cross-phase modulation in Bragg gratings. *Phy.Rev. A* 1994, **50**(4)**:** 3447-3452.

60. Gordon JP. Dispersive perturbations of solitons of the nonlinear Schrödinger equation. *J. Opt. Soc. Am. B* 1992, **9**(1)**:** 91-97.

61. Yulin AV, Skryabin DV, Russell PSJ. Four-wave mixing of linear waves and solitons in fibers with higher-order dispersion. *Opt. Lett.* 2004, **29**(20)**:** 2411-2413.

62. Skryabin DV, Yulin AV. Theory of generation of new frequencies by mixing of solitons and dispersive waves in optical fibers. *Phy.Rev. E* 2005, **72**(1)**:** 016619.

63. de Sterke CM, Broderick NGR, Eggleton BJ, Steel MJ. Nonlinear Optics in Fiber Gratings. *Opt. Fiber Technol.* 1996, **2**(3)**:** 253-268.

64. Reed EJ, Soljačić M, Joannopoulos JD. Color of Shock Waves in Photonic Crystals. *Phys. Rev. Lett.* 2003, **90**(20)**:** 203904.

65. Reed EJ, Soljačić M, Joannopoulos JD. Reversed Doppler Effect in Photonic Crystals. *Phys. Rev. Lett.* 2003, **91**(13)**:** 133901.

66. Stepanov NS. Waves in nonstationary media. *Radiophysics and Quantum Electronics* 1993, **36**(7)**:** 401-409.

67. Plansinis BW, Donaldson WR, Agrawal GP. Temporal waveguides for optical pulses. *J Opt Soc Am B* 2016, **33**(6)**:** 1112-1119.

68. Tanabe T, Nishiguchi K, Shinya A, Kuramochi E, Inokawa H, Notomi M*, et al.* Fast all-optical switching using ion-implanted silicon photonic crystal nanocavities. *Appl.Phys. Lett.* 2007, **90**(3)**:** 031115.

69. Zhang Y, Husko C, Lefrancois S, Rey IH, Krauss TF, Schröder J*, et al.* Non-degenerate two-photon absorption in silicon waveguides: analytical and experimental study. *Opt. Exp.* 2015, **23**(13)**:** 17101-17110.

70. Joannopoulos JD. Photonic Crystals, Molding the Flow of Light Princeton University Press; 2008.

71. Yanik MF, Fan S. Stopping and storing light coherently. *Phy.Rev. A* 2005, **71**(1)**:** 013803.

72. Preble SF, Xu Q, Lipson M. Changing the colour of light in a silicon resonator. *Nat. Photon.* 2007, **1**(5)**:** 293-296.

73. Kampfrath T, Beggs DM, White TP, Melloni A, Krauss TF, Kuipers L. Ultrafast adiabatic manipulation of slow light in a photonic crystal. *Phy.Rev. A* 2010, **81**(4)**:** 043837.

74. Munoz MC, Kanchana A, Petrov AY, Eich M. Dynamic Light Storage in Slow Light Waveguides. *IEEE J. Quantum Electron.* 2012, **48**(7)**:** 862-866.

75. Verbist M, Bogaerts W, Thourhout DV. Design of Weak 1-D Bragg Grating Filters in SOI Waveguides Using Volume Holography Techniques. *J. Lightwave Technol.* 2014, **32**(10)**:** 1915-1920.

76. Li J, White TP, O'Faolain L, Gomez-Iglesias A, Krauss TF. Systematic design of flat band slow light in photonic crystal waveguides. *Opt. Exp.* 2008, **16**(9)**:** 6227-6232.

77. Dudley JM, Genty G, Coen S. Supercontinuum generation in photonic crystal fiber. *Rev. Mod. Phys.* 2006, **78**(4)**:** 1135-1184.

78. Meltz G, Morey WW, Glenn WH. Formation of Bragg gratings in optical fibers by a transverse holographic method. *Opt. Lett.* 1989, **14**(15)**:** 823-825.

79. Yanik MF, Fan S. Time Reversal of Light with Linear Optics and Modulators. *Phys. Rev. Lett.* 2004, **93**(17)**:** 173903.

80. Sivan Y, Pendry JB. Time Reversal in Dynamically Tuned Zero-Gap Periodic Systems. *Phys. Rev. Lett.* 2011, **106**(19)**:** 193902.

81. Yachini M, Malomed B, Bahabad A. Envelope Time Reversal of Optical Pulses Following Frequency Conversion with Accelerating Quasi-Phase-Matching. *ACS Photonics* 2016, **3**(11)**:** 2017-2021.

82. Minkov M, Fan S. Localization and time-reversal of light through dynamic modulation. *Phy.Rev. B* 2018, **97**(6)**:** 060301.

83. Konoike R, Asano T, Noda S. On-chip dynamic time reversal of light in a coupled-cavity system. *APL Photonics* 2019, **4**(3)**:** 030806.

84. Colman P, Combrié S, Lehoucq G, de Rossi A, Trillo S. Blue Self-Frequency Shift of Slow Solitons and Radiation Locking in a Line-Defect Waveguide. *Phys. Rev. Lett.* 2012, **109**(9)**:** 093901.

85. Blanco-Redondo A, Husko C, Eades D, Zhang Y, Li J, Krauss TF*, et al.* Observation of soliton compression in silicon photonic crystals. *Nat. Commun.* 2014, **5:** 3160.

86. Yulin AV, Skryabin DV. Slowing down of solitons by intrapulse Raman scattering in fibers with frequency cutoff. *Opt. Lett.* 2006, **31**(21)**:** 3092-3094.

87. Demircan A, Amiranashvili S, Steinmeyer G. Controlling Light by Light with an Optical Event Horizon. *Phys. Rev. Lett.* 2011, **106**(16)**:** 163901.

88. Belgiorno F, Cacciatori SL, Clerici M, Gorini V, Ortenzi G, Rizzi L*, et al.* Hawking Radiation from Ultrashort Laser Pulse Filaments. *Phys. Rev. Lett.* 2010, **105**(20)**:** 203901.

89. Plansinis BW, Donaldson WR, Agrawal GP. Cross-phase-modulation-induced temporal reflection and waveguiding of optical pulses. *J. Opt. Soc. Am. B* 2018, **35**(2)**:** 436-445.

90. Gaeta AL, Lipson M, Kippenberg TJ. Photonic-chip-based frequency combs. *Nat. Photon.* 2019, **13**(3)**:** 158-169.

91. Köttig F, Novoa D, Tani F, Günendi MC, Cassataro M, Travers JC*, et al.* Mid-infrared dispersive wave generation in gas-filled photonic crystal fibre by transient ionization-driven changes in dispersion. *Nat. Commun.* 2017, **8**(1)**:** 813.

92. Maier SA. *Plasmonics: Fundamentals and Applications*. Springer US, 2007.

93. Stockman MI. Nanofocusing of Optical Energy in Tapered Plasmonic Waveguides. *Phys. Rev. Lett.* 2004, **93**(13)**:** 137404.

94. Gramotnev DK, Bozhevolnyi SI. Nanofocusing of electromagnetic radiation. *Nat. Photon.* 2013, **8:** 13.

95. Willner AE, Khaleghi S, Chitgarha MR, Yilmaz OF. All-Optical Signal Processing. *J. Lightwave Technol.* 2014, **32**(4)**:** 660-680.

96. Wengerowsky S, Joshi SK, Steinlechner F, Hübel H, Ursin R. An entanglement-based wavelength-multiplexed quantum communication network. *Nature* 2018, **564**(7735)**:** 225-228.

97. Leuthold J, Koos C, Freude W. Nonlinear silicon photonics. *Nat. Photon.* 2010, **4:** 535.

98. Morichetti F, Canciamilla A, Ferrari C, Samarelli A, Sorel M, Melloni A. Travelling-wave resonant four-wave mixing breaks the limits of cavity-enhanced all-optical wavelength conversion. *Nat. Commun.* 2011, **2:** 296.

99. Monat C, Ebnali-Heidari M, Grillet C, Corcoran B, Eggleton BJ, White TP*, et al.* Four-wave mixing in slow light engineered silicon photonic crystal waveguides. *Opt. Exp.* 2010, **18**(22)**:** 22915-22927.

100. Suchowski H, Porat G, Arie A. Adiabatic processes in frequency conversion. *Laser Photonics Rev.* 2014, **8**(3)**:** 333-367.

101. Tan DTH, Agarwal AM, Kimerling LC. Nonlinear photonic waveguides for on-chip optical pulse compression. *Laser Photonics Rev.* 2015, **9**(3)**:** 294-308.

102. Foster MA, Salem R, Okawachi Y, Turner-Foster AC, Lipson M, Gaeta AL. Ultrafast waveform compression using a time-domain telescope. *Nat. Photon.* 2009, **3:** 581.

103. Karpiński M, Jachura M, Wright LJ, Smith BJ. Bandwidth manipulation of quantum light by an electro-optic time lens. *Nat. Photon.* 2016, **11:** 53.

104. Xu Q, Dong P, Lipson M. Breaking the delay-bandwidth limit in a photonic structure. *Nat. Phys.* 2007, **3**(6)**:** 406-410.

105. Phillips DF, Fleischhauer A, Mair A, Walsworth RL, Lukin MD. Storage of Light in Atomic Vapor. *Phys. Rev. Lett.* 2001, **86**(5)**:** 783-786.

106. Liu C, Dutton Z, Behroozi CH, Hau LV. Observation of coherent optical information storage in an atomic medium using halted light pulses. *Nature* 2001, **409:** 490.

107. Tanaka Y, Upham J, Nagashima T, Sugiya T, Asano T, Noda S. Dynamic control of the Q factor in a photonic crystal nanocavity. *Nat. Mater.* 2007, **6**(11)**:** 862-865.

108. Tanabe T, Notomi M, Taniyama H, Kuramochi E.Dynamic release of trapped light from an ultrahigh-Q nanocavity via adiabatic frequency tuning. *Phys. Rev. Lett.* 2009, **102**(4)**:** 043907.

109. Elshaari AW, Aboketaf A, Preble SF. Controlled storage of light in silicon cavities. *Opt. Exp.* 2010, **18**(3)**:** 3014-3022.

110. Upham J, Inoue H, Tanaka Y, Stumpf W, Kojima K, Asano T*, et al.* Pulse capture without carrier absorption in dynamic Q photonic crystal nanocavities. *Opt. Exp.* 2014, **22**(13)**:** 15459-15466.

111. Drori J, Rosenberg Y, Bermudez D, Silberberg Y, Leonhardt U. Observation of Stimulated Hawking Radiation in an Optical Analogue. *Phys. Rev. Lett.* 2019, **122**(1)**:** 010404.